Comparison of Subjective and Objective Methods of Corneoscleral Limbus Identification from Anterior Segment Optical Coherence Tomography Images

COMPARISON OF SUBJECTIVE AND OBJECTIVE METHODS OF CORNEOSCLERAL LIMBUS IDENTIFICATION FROM ANTERIOR SEGMENT OCT IMAGES

MARTA K. SKROK, MSC[1,*], DAVID ALONSO-CANEIRO, PHD[2], JOANNA PRZEŹDZIECKA-DOŁYK, MD, PHD[1,3] AND DAMIAN SIEDLECKI, PHD[1]

[1]Wroclaw University of Science and Technology, Visual Optics Group, Department of Optics and Photonics, Wybrzeże Wyspiańskiego 27, 50-370 Wrocław, Poland
[2]Queensland University of Technology, Contact Lens and Visual Optics Laboratory, School of Optometry and Vision Science, Victoria Park Road, Kelvin Grove QLD 4059, Brisbane, Australia
[3]Wroclaw Medical University, Department of Ophthalmology, ul. Borowska 213, 55-556 Wrocław, Poland

**marta.skrok@pwr.edu.pl*
* Wybrzeże Wyspiańskiego 27, 50-370 Wrocław, Poland

The manuscript contains 3843 words, 5 figures, 4 tables, 37 references and 2 Appendices.

SIGNIFICANCE

This study evaluates the reliability and validity of an automatic method of the external and internal limbal points identification from anterior segment OCT images in comparison to manual delineation.

PURPOSE

The purpose of this work is to evaluate the repeatability and precision of a previously proposed automatic method of external and internal limbal points identification and to compare them to the manual delineation by experienced clinicians in terms of limbus diameter.

METHODS

OCT tomograms obtained for 12 healthy volunteers without a history of eye diseases were analyzed. 15 OCT tomograms were captured for each patient. For all the images, the external and internal limbal

points were determined using both the automatic and manual methods. The external and internal limbus diameters were used as the comparative parameter between the methods under consideration. The statistical analysis included mean, standard deviation, the Passing-Bablok regression and the Pearson correlation coefficient.

RESULTS

A strong linear dependence between the automatic and manual methods was identified. While compared to the subjective estimates from clinicians, the automatic technique overestimated the external limbus diameter (bias equals 0.21 mm for optometrist and 0.23 mm for ophthalmologist) and slightly underestimated the internal limbus diameter (bias equals 0.13 mm for optometrist and 0.04 mm for ophthalmologist). The automatic method showed significantly better repeatability than the manual method in the case of external limbal points identification, and comparably high repeatability for internal limbal points recognition.

CONCLUSIONS

Due to high precision and excellent repeatability, the automatic method of limbal points identification may be successfully used for estimation of the dynamic changes in the geometry of the anterior segment of the eye, where the large number of captured OCT images need to be processed automatically with high precision.

1. Introduction

There are several structures located in the limbal area, which are crucial for the proper functioning of the eye and the entire visual system. The corneoscleral limbus contains limbal stem cells, which play an important role in the process of regeneration of the corneal epithelium.[1] It is also a natural barrier which prevents the penetration of the cells to the epithelium and blood vessels for conjunctiva into the cornea.[2]

Determining the position of the corneoscleral limbus can be important for a number of clinical and research tasks, including contact lenses fitting. [3] The proper fit of the contact lenses is determined on the basis of the distance of the edge of the contact lens from the corneoscleral limbus. [3] The posterior limbus is also of particular importance for proper estimation of the iridocorneal angle in the diagnostics of angle-closure glaucoma.[4] Also angle-to-angle distance, associated with the posterior limbus localization, is one of the factors used for anterior chamber phakic intraocular lens (pIOL) power calculations.[5]

A crucial element in the process of determining both the anterior and posterior corneal diameters is the reliable and precise localization of the corneoscleral limbus on both the anterior and posterior surfaces of the cornea. The limbus is the transition area connecting the light-transparent cornea with the opaque sclera and conjunctiva. The limbal area is restricted by four characteristic points (see Fig. 1 for notation): the peripheral point of the Vogt's palisade (1), the most peripheral point of Bowman's layer (2), the peripheral point of the corneal endothelium (3) and the scleral spur (4). The segment between points (1) and (2) is noted as anterior limbus, while the segment between points (3) and (4) is noted as posterior limbus.[6]

A variety of methods for estimation of the corneal or limbal diameters can be found in the literature. One of the basic methods is to measure white-to-white distance. It involves measuring the horizontal visible iris diameter (HVID), based on a visual assessment using a scanning slit topography or videokeratometry.[7] This method, due to its simplicity, is widely used in clinical practice. However, previous work has shown that the correlation between HVID and the actual location of the corneoscleral limbus can be weak, probably due to peripheral corneal opacities such as arcus senilis.[8] Another method, based on the anatomical structure and optical properties of the anterior segment, is to analyze the gradient of brightness on the images of the cornea captured with use of videokeratoscope[9] or a simple camera,[10] however due to the imaging technique these methods can only estimate the anterior limbus properties.

An alternative method to estimate the anterior limbus is based on the analysis of the geometry, such as radius of curvature of the outer surface of the eye, within the region of junction between the cornea and sclera.[11] In this case, the corneoscleral limbus is located in the position where the radius of curvature changes rapidly. It is also possible to locate the corneoscleral limbus by analyzing the structure of the cornea, using the images obtained from fluorescence microscopy[12] or optical coherence tomography (OCT).[13] This method involves manual identification of the structures forming the corneoscleral limbus in the images, which makes it unsuitable for processing large datasets.

OCT has been extensively used in clinical ophthalmic practice for almost three decades. This technique allows quick, and non-invasive examination of the ocular tissue, providing a high-resolution cross-sectional (or volumetric) images. Several studies showed that it enables precise assessment of the parameters of individual structures of anterior eye,[14] contact lens fitting,[15,16] the iridocorneal angle for glaucoma diagnosis,[17] in diagnosis of keratoconus,[18] as well as to evaluate the structures of the anterior segment of the eye before and after laser refractive surgery and implanting a phakic intraocular lens.[19]

In the present study we evaluate a fully automatic method to estimate the corneoscleral limbal points on OCT images of the full width of the anterior segment of the eye. The superior axial and lateral resolution of the OCT technology,[20] makes it an ideal imaging tool for precise estimation of the geometry of the cornea, as well as the whole anterior chamber. The method, which was partly described in the conference paper,[21] incorporates a geometrical analysis of the shape of the cornea and corneoscleral junction to extract the points of interest (see Figure 1 for notation): external limbal point (5) on the anterior ocular surface, and internal limbal point (3). The internal limbal point, associated with scleral spur, is widely accepted as one of the boundaries of the limbus. While the external limbal point needs a short explanation.

Bergmanson and colleagues[22] stated that the exact estimation of limbus boundaries is not straightforward and therefore there is a lack of precise methods for determining the limbal width or the

limbus-to-limbus distance. The external limbal point (5), estimated by the automatic method,[21] was chosen as the landmark associated with the location where the local curvature of the anterior ocular surface changes its sign[11]. Physiologically, this point is located within the limbal area between points (1) and (2) (see Figure 1). Given that these points can be easily localized by means of automated analytical methods, which are independent from the observer, there is a potential for developing new protocols for determining the dimensions of the limbus.

In this study, a detailed statistical validation of the automatic method is presented. The proposed technique is validated in detail against two experienced observers that identify the limbal points. Also the discrepancies between the methods are explained and the usefulness of the automatic method for the purposes of estimation of the dynamic changes in the anterior segment geometry is discussed.

2. Methods

2.1. Human Subjects Protection

All subjects taking part in the present study were informed about the protocol, they agreed to participate in the study and signed an informed consent form. Experimental protocol was approved by the Institutional Board of the Department of Ophthalmology, Wroclaw Medical University. The study was registered by the number of NCT03906279 and conducted by the Department of Optics and Photonics, Wroclaw University of Science and Technology, in cooperation with the Department of Ophthalmology, Wroclaw Medical University.

2.2. OCT instrument

An anterior segment swept source OCT instrument, Casia 2 (Tomey Corporation, Japan) was used in this study. It uses a tunable light source with a central wavelength λ = 1310 nm and allows to capture the OCT data with the acquisition rate of 50000 A-scans per second. This long wavelength ensures a greater sensitivity and better tissue penetration, which is of particular importance for imaging the internal

structures of the anterior segment of the eye, such as iris, sclera and iridocorneal angle. The line scanning protocol in the horizontal meridian thru the corneal center was used to collect the data in the current study.

The raw data obtained from the device correspond with the image of the whole anterior segment of the subject's eye of a size 1996 × 1745 pixels. Taking into account the manufacturer specifications: the scan depth of 11 mm and the lateral scan range of 16 mm, the digital axial and transversal resolutions were estimated to be 8.5 μm (in tissue) and 8 μm, respectively. An exemplary tomogram is presented in Fig. 2a. After data acquisition, the OCT images were automatically segmented: including the anterior and posterior cornea, iris and anterior crystalline lens boundaries in order to be associated to relevant anatomical surfaces.[23] Boundary profiles were smoothed by a custom developed procedure (details in Ref.[24]) and finally corrected from optical distortion by means of a custom procedure (see Fig. 2b).[25]

2.3. Participants

We used OCT data obtained from 12 healthy volunteers, aged from 22 to 48 years old, 8 females and 4 males. The measurements were taken from 7 left eyes and 5 right eyes. Fifteen different scans of the anterior segment of the same eye were captured during a single visit for each participant. Then, each of the OCT images was processed in order to identify both the external and internal limbal points. From the obtained limbus points localized at the anterior ocular surface, the values of both external limbus diameter (further referred to as *ELD*) were calculated as the Euclidean distance between the two external limbal points. Similarly, and internal limbus diameter (further referred to as *ILD*) were calculated as the Euclidean distance between the two internal limbal points identified at the posterior corneal surface.

2.4. Automatic localization methods of external and internal limbal points

In a previous publication[21], we introduced two versatile methods of corneoscleral limbus estimation from OCT images of the whole anterior segment of the eye, based on geometrical dependencies on shape of cornea and corneoscleral junction.

Briefly, the first method locates the external limbal point at the anterior ocular surface by using the estimation of the local radii of curvature (or curvature) along the whole anterior ocular surface. The details on how the local curvature can be estimated for the discrete set of data points can be found in Appendix 1. According to the literature,[26] the radius of curvature changes abruptly at the junction point of the cornea and sclera/conjunctiva, creating the anterior scleral sulcus. The external limbal point can be identified as the point, where the local curvature (reciprocal of local radius of curvature) reaches the value of zero. By looking at the curvature profile of the anterior surface of the eye, this point can be clearly identified (Fig. 3a).

The second method estimates the location of the internal limbal point at the posterior surface of the cornea and sclera. It uses the estimation of actual thickness profile of the cornea calculated as the distance between the two corneal surfaces taken along the normal to the anterior surface. The profile of the thickness manifests two superior local maxima (see Fig. 3b), which can be associated with the location of internal limbal points. To be precise, these maxima directly indicate points at the anterior corneal surface, and the positions of posterior limbal points need to be calculated as the maximum distances taken along the line perpendicular to the anterior corneal surface at these points. According to the literature,[27] these internal limbal points can be identified as the tip of the scleral spur. Finally, the *ELD* and the *ILD* estimates were estimated from these points.

2.5. Statistical analysis

The automatic methods were statistically validated, with regards to external and internal limbal diameters, by comparing the automatic with the subjective method of identification. The manual limbal points identification was performed by two clinicians: an ophthalmologist with significant experience in

the analysis of OCT image of the anterior segment (Operator A) and an optometrist (Operator B) that had no experience in this task and was instructed by Operator A on the image marking criteria. The operators, which were both masked to the automatic method predictions, were instructed to subjectively estimate the positions of (a) the external limbal points at the boundary points of Bowman's layer and (b) internal limbal points at the scleral spur, at each side of the cornea. The tomograms were randomly presented to the both operators. The subjective data from each side of the cornea was processed in order to calculate both *ELD* and *ILD* for each single tomogram.

The Passing-Bablok regression was used in order to compare the results obtained by means of both automated and the two manual methods, this non-parametric method of linear regression is recommended when comparing the two data sets that are estimated with some errors.[28] The Pearson correlation coefficient was also calculated in order to measure the strength of the linear relationship between each pair of method.

Intravisit reproducibility was defined as the reproducibility of limbal diameter estimation obtained by limbal points identification made by a single observer on the measurement session (15 times for each subject). Interobserver reproducibility was defined as the reproducibility of limbal diameter estimation obtained by limbal points identification made by both human observers and automated delineation for the same measurement session. The bias or average agreement was assessed for each pair of subjective and automated delineation by calculating the mean difference in limbal diameter estimation. This was reported with 95% confidence intervals (95% *CI*).

MedCalc 19 statistical software (MedCalc Software, Ostend, Belgium) was used for the statistical analysis.

3. Results

The results presented in Table 1 show the difference between the points obtained from manual processing and those from the automatic analysis. In terms of distances from the points obtained by the automatic

analysis, the discrepancies are 3 times larger for the external limbus than for the internal limbus. The significance test showed that there are no significant differences between operators for the internal limbal points – both for nasal and temporal sides, while for the external limbal points the results of manual processing by the same operator show statistically significant differences for both nasal and temporal sides (see Table 2). Tables 3 and 4 present detailed statistical analysis of the results of anterior and posterior limbal diameter estimation obtained by means of both automatic and subjective methods.

The statistical analysis proved that this linear correlation for both external and internal diameter is strong but there is some bias between the results obtained by means of automatic and manual methods (r = 0.89, 95 % CI: 0.85-0.92 and r = 0.89, 95 % CI: 0.86-0.92 when one compares *ELD* and *ILD,* respectively, between the results obtained by Operator B and the automatic method, and r = 0.84, 95 % CI: 0.77-0.87 and r = 0.86, 95 % CI: 0.82-0.89 when one compares, respectively, *ELD* and *ILD* results obtained by between Operator A and the automatic method).

The Passing-Bablok regression showed that there exists a strong correlation between the results obtained by means of both manual and automatic methods (see Fig. 4). This correlation between the automatic and manual methods is particularly clear for *ILD*, for which the slope is 0.911, 95% CI: 0.842-0.986 between the results obtained by the Operator A and the automatic method and 0.931, 95% CI: 0.862-1.004 between the results obtained by the Operator B and the automatic method.

The Bland-Altman analysis for non-parametric data showed some bias between the manual and automatic processing. *ELD* by means of automatic method seems to be overestimated by 0.235 mm (with the total width of 95% CI equal to 0.188 mm) in comparison to the results obtained for Operator A and by 0.207 mm (with the total width of 95% CI equal to 0.152 mm) in comparison to the results obtained for Operator B. Regarding the *ILD* obtained with use of automatic method, it seems to be underestimated by only 0.041 mm (with the total width of 95% CI equal to 0.175 mm) in comparison to the results obtained

for Operator A and by 0.134 mm (with the total width of 95% confidence interval equal to 0.213 mm) in comparison to the results obtained for Operator B.

4. Discussion and conclusions

This study presented and evaluated an automatic method to estimate the external and internal limbal points from OCT images based in the shape of the tissue. The results presented in Table 1 show the difference between the points obtained from manual processing and those from the automatic analysis. In terms of distances from the points obtained by automatic analysis, the discrepancies are 3 times larger for the external limbus than for the internal limbus. The significance test showed that there are no significant differences between operators for the internal limbal points – both for nasal and temporal sides, while for the external limbal points the results of manual processing by the same operator show statistically significant differences for both nasal and temporal sides (see Table 2).

The results of statistical analysis of the limbal diameter estimation showed the presence of some bias between the results obtained while comparing the proposed automatic method and the subjective estimation (see Tables 3 and 4, and Fig. 4). To summarize, the automatic technique overestimated the *ELD* and underestimated the *ILD*, while compared to the subjective estimates of both an Operator A and Operator B. This difference is likely due to the way the observers selected the points, taking into account that, in particular, the human operators identified the limbal points based on their anatomical background and the whole OCT tomogram. While the automatic method relies on precise segmentation[23] and uses only the geometrical dependencies of the shape of the cornea and sclera. Effectively, the automatic method identified slightly different locations than the human operators, particularly manifested in the case of *ELD*. In comparison to the automatic method, *ELD* is underestimated by 0.21 mm for Operator B and by 0.24 mm for Operator A (see Appendix Figure A1 for details of non-parametric Bland-Altman analysis). The automatic method underestimates the *ILD* by only 0.04 mm and 0.13 mm in comparison to the Operator A and Operator B, respectively. Fig. 5 presents the exemplary results of limbal points

estimation by means of both manual and automatic methods. Most of the studies[11,29,30] aiming to compare different methods of corneal or limbal diameter estimations report comparable or even larger discrepancies to the ones obtained in this study. It is worth noting that imaging modalities and parameter definition may be slightly different between the studies, that include metrics such as white-to-white (WTW), angle-to-angle (ATA) diameters or horizontal visual iris diameter (HVID). For example, Kohnen et al.[29] compared WTW distance (from Orbscan and IOLMaster devices) and ATA diameter (from Visante OCT) and found the differences ranging from 0.32 to 0.68 mm. Baumeister et al.[30] compared 5 different methods, both manual and automatic, and their results showed discrepancies between the mean results ranging from 0.07 to 0.45 mm. Additionally, they found differences up to 0.5 mm between the diameters obtained by two operators of the instrument. Therefore, the relative difference between the manual and automatic methods reported in this work, ranging from 0.21 to 0.24mm for *ELD*, and from 0.04 to 0.13 mm for *ILD* seems to be acceptable both for research and clinical applications.

Despite the small discrepancies between the subjective and automatic results, the detailed statistical analysis presented in the previous section showed that the automatic method of external limbal points identification provides more precise results than the manual processing. This is due to objective analysis of the numerical data, whilst results obtained by human operators may be affected by the error associated with visual assessment of the gray level changes in the raw tomograms, subjective assessment as well as monitor resolution and external illumination level. The presented results showed that the observers clinical experience in manual processing of the anterior chamber tomographic images plays a significant role in precision and repeatability of subjective assessment. Moreover, since the statistical analysis was performed on the series of 15 different images captured for each subject, the automatic limbal points localization method seems to be independent of small, involuntary rotational movements of the subject's eye and provide precise, stable results.

In the case of internal limbal points, the automatic method of identification provides significantly better repeatability than the manual identification by Operator B, whilst in relation to the localization obtained by the experienced Operator A, the automatic processing provides results of comparable repeatability. This is due to the fact that unlike the external limbal points, the internal limbal points (recognized as the tip of the scleral spur, see Fig. 1) can be visually estimated with ease. Therefore the obtaining the same or comparable repeatability as the experienced ophthalmologist seem a reasonable results.

Although in 2017 Bergmanson and Martinez[22] claimed that "with current OCT instruments it is difficult to obtain a high resolution limbus-to-limbus single field of view", it is work noting that state-of-the-art clinical OCT instrument provide an excellent trade-off between transverse resolution of the corneal data and the lateral/axial imaging range. The instrument used in the present study allows to capture whole anterior segment images with a lateral range of 16 mm and the transversal digital resolution less than 8 microns in tissue. This resolution compares favorably with previous method use to extract limbal diameter and should provide sufficient detail to reconstruct the limbal area.

The main limitations of the present study is that the anterior segment OCT images were acquired in a small sample size of only healthy participants. Thus, all the results presented for the automatic methods were obtained from OCT images of healthy young participants. The precision of segmentation, and subsequently the result presented here, strongly depends on the OCT image quality or to be more precise by the signal-to-noise parameter. To further validate the method future studies should expand the validation of the automatic method on larger population containing both normal subjects and patients with anterior segment conditions, such as angle-closure glaucoma[4] or keratoconic or post-refractive surgery corneas[31-33] or older participants. For patients with severe pathologies that significantly affect the anterior or posterior corneal shapes (such as edematous corneas, bullous keratopathy, and acute corneal hydrops[34,35]), the proposed method may fail.

The other limitation of the current work is that the OCT images were taken at a single meridian (horizontal). The anterior chamber geometry, including the limbus shapes, is known to change shape in different meridians.[36,37] Future work should investigate the effect of meridian on the proposed method.

A method to extract the external and internal limbal points was evaluated against two clinicians with different level of experience in the manual segmentation task. Although small differences between manual and automatic method were observed, those differences are likely connected to the different principles of detection rather than a limitation of the proposed method. It is worth noting that these differences are still smaller that the method's variability. The precision of the proposed methods was comparable or superior to the manual analysis. The automatic nature of the numerical method combined with the repeatability and stability of the results, makes the proposed tool suitable for the automatic estimation of the limbus. These advantages may be of particular interest for application of this method in the estimation of the dynamic changes in the anterior segment of the eye, i.e. rapid fluctuation of the iridocorneal angle, where the large number of captured OCT images need to be processed automatically with a superior precision.

Table 1. The comparison of external and internal nasal and temporal limbal points localization by means of human operators estimated as the distance difference (in mm) between the results of manual minus automatic processing. The table presents the average of the mean and standard deviation values obtained from a series of 15 images captured for all 12 subjects.

	Operator A – automatic method				**Operator B – automatic method**			
	Temporal limbal point		**Nasal limbal point**		**Temporal limbal point**		**Nasal limbal point**	
	Mean [mm]	std dev [mm]	Mean [mm]	std dev [mm]	Mean [mm]	std dev [mm]	Mean [mm]	std dev [mm]
External limbus	**0.139**	**0.072**	**0.322**	**0.105**	**0.125**	**0.079**	**0.300**	**0.114**
Internal limbus	**0.103**	**0.049**	**0.134**	**0.060**	**0.115**	**0.070**	**0.135**	**0.071**

std dev = standard deviation

Table 2. Result of test of significance (p-values) between the results of limbal points localization on both the temporal and nasal sides of the eye and localization by means of human operators for with automatic estimation taken as reference. The values are presented for both external and internal limbal points. The underlined values note that there exist significant differences between obtained results.

External limbus				
	Operator A temporal	**Operator A nasal**	**Operator B temporal**	**Operator B nasal**
Operator A temporal	x	<u><0.001</u>	0.637	<u><0.001</u>
Operator A nasal	<u><0.001</u>	x	<u><0.001</u>	0.67
Operator B temporal	0.637	<u><0.001</u>	x	<u><0.001</u>
Operator B nasal	<u><0.001</u>	0.67	<u><0.001</u>	x
Internal limbus				
	Operator A temporal	**Operator A nasal**	**Operator B temporal**	**Operator B nasal**
Operator A temporal	x	0.173	0.976	0.475
Operator A nasal	0.173	x	0.211	0.623
Operator B temporal	0.976	0.211	x	0.492
Operator B nasal	0.475	0.623	0.492	x

Table 3. Per subject and group estimates of the *ELD*. Each column presents the mean and standard deviation of two manual operators and automatic corneoscleral limbus identification.

	Operator A		**Operator B**		**Automatic method**	
Subject	Mean *ELD* [mm]	std dev [mm] (range)	Mean *ELD* [mm]	std dev [mm] (range)	Mean *ELD* [mm]	std dev [mm] (range)
1	11.48	0.079 (11.34-11.60)	11.54	0.122 (11.33-11.74)	11.66	0.038 (11.56-11.70)
2	11.22	0.093 (11.09-11.37)	11.36	0.091 (11.22-11.50)	11.60	0.040 (11.53-11.67)
3	11.73	0.082 (11.61-11.89)	11.97	0.120 (11.68-12.10)	11.99	0.040 (11.92-12.05)
4	11.84	0.098 (11.61-11.96)	11.69	0.087 (11.52-11.80)	11.85	0.067 (11.69-11.98)
5	11.42	0.070 (11.28-11.51)	11.62	0.099 (11.44-11.80)	12.14	0.043 (12.07-12.20)
6	12.54	0.097 (12.41-12.77)	12.78	0.115 (12.52-12.98)	13.18	0.082 (13.00-13.31)
7	12.19	0.075 (12.03-12.30)	12.09	0.079 (11.94-12.25)	12.39	0.063 (12.30-12.54)
8	11.66	0.081 (11.43-11.75)	11.70	0.130 (11.54-11.95)	11.59	0.029 (11.54-11.64)
9	11.78	0.106 (11.63-11.97)	11.93	0.055 (11.83-12.02)	12.06	0.026 (12.02-12.09)
10	11.95	0.071 (11.80-12.02)	11.93	0.066 (11.79-12.02)	12.11	0.106 (11.98-12.29)
11	11.99	0.051 (11.92-12.09)	12.13	0.066 (12.05-12.23)	12.34	0.035 (12.30-12.40)
12	11.78	0.108 (11.55-11.90)	11.77	0.072 (11.63-11.88)	11.98	0.046 (11.92-12.10)
All subjects	11.80	0.84	11.88	0.092	12.07	0.051

ELD = external limbal diameter; std dev = standard deviation.

Table 4. Per subject and group estimates of the *ILD*. Each column presents the mean and standard deviation of two manual operators and automatic corneoscleral limbus identification.

	Operator A		**Operator B**		**Automatic method**	
Subject	Mean *ILD* [mm]	std dev [mm] (range)	Mean *ILD* [mm]	std dev [mm] (range)	Mean *ILD* [mm]	std dev [mm] (range)
1	11.09	0.048 (11.00-11.17)	11.20	0.067 (11.03-11.33)	11.24	0.035 (11.20-11.30)
2	11.15	0.071 (11.04-11.31)	11.31	0.111 (11.17-11.52)	11.22	0.055 (11.16-11.39)
3	11.41	0.062 (11.26-11.51)	11.55	0.096 (11.29-11.68)	11.46	0.032 (11.40-11.50)
4	12.01	0.078 (11.91-12.15)	12.10	0.108 (11.89-12.27)	12.07	0.028 (12.03-12.12)
5	11.91	0.062 (11.82-12.04)	11.80	0.114 (11.59-11.98)	11.56	0.069 (11.45-11.67)
6	12.03	0.034 (11.95-12.08)	12.24	0.095 (12.04-12.42)	12.06	0.099 (11.92-12.20)
7	11.82	0.047 (11.75-11.93)	11.93	0.075 (11.80-12.07)	11.77	0.067 (11.64-11.85)
8	11.04	0.045 (10.95-11.11)	11.21	0.043 (11.14-11.29)	10.85	0.075 (10.71-10.99)
9	11.97	0.064 (11.88-12.09)	12.07	0.068 (11.97-12.17)	11.94	0.024 (11.91-11.98)
10	11.70	0.050 (11.63-11.79)	11.77	0.045 (11.72-11.88)	11.65	0.029 (11.61-11.69)
11	11.51	0.034 (11.47-11.60)	11.61	0.063 (11.54-11.74)	11.53	0.053 (11.43-11.58)
12	12.11	0.040 (12.04-12.17)	12.17	0.034 (12.12-12.24)	12.07	0.028 (12.02-12.12)
All subjects	11.65	0.053	11.75	0.077	11.70	0.50

ILD = internal limbal diameter; std dev = standard deviation.

Acknowledgments

The authors would like to thank Magdalena Widlicka for her helpful advice regarding the statistical analysis.

Disclosures

The authors declare no conflicts of interest.

Appendix

Appendix 1. Description on how the local curvature can be estimated for the discrete set of data points obtained from OCT data processing (segmentation). This description should give an overview of the local corneal curvature calculation and should be helpful in implementation of the automatic method of limbal points localization on the anterior surface of the cornea to the custom processing software.

Appendix Figure A1. Results of Bland-Altman analysis. Agreement for *ELD* (A and B) and *ILD* (C and D) compared for measurements obtained by means of automatic method and manual processing by human operators. The bias (median) is marked as a solid red line. The 95% confidence intervals of the bias are shown as dashed red lines. The limits of agreement are shown as solid black lines. The values of particular parameters are listed within each plot.

References

1. Collinson JM, Chanas SA, Hill RE, West JD. Corneal Development, Limbal Stem Cell Function, and Corneal Epithelial Cell Migration in the Pax6(+/-) Mouse. Invest Ophthalmol Vis Sci 2004;45:1101–8.
2. Gaudana R, Ananthula HK, Parenky A, Mitra AK. Ocular Drug Delivery. AAPS J 2010;12:348–60.
3. Hall LA, Young G, Wolffsohn JS, Riley C. The Influence of Corneoscleral Topography on Soft Contact Lens Fit. Invest Ophthalmol Vis Sci 2011;52:6801–6.
4. Sakata LM, Lavanya R, Friedman DS, et al. Comparison of Gonioscopy and Anterior Segment Ocular Coherence Tomography in Detecting Angle Closure in Different Quadrants of the Anterior Chamber Angle. Ophthalmology 2008;115:769–74.
5. Güell JL, Morral M, Kook D, Kohnen T. Phakic Intraocular Lenses Part 1: Historical Overview, Current Models, Selection Criteria, and Surgical Techniques. J Cataract Refract Surg 2010;36:1976–93.
6. McGowan SL, Edelhauser HF, Pfister RR, Whikehart DR. Stem Cell Markers in the Human Posterior Limbus and Corneal Endothelium of Unwounded and Wounded Corneas. Mol Vis 2007;13:1984–2000.

7. Hall LA, Hunt C, Young G, Wolffsohn J. Factors Affecting Corneoscleral Topography. Invest Ophthalmol Vis Sci 2013;54:3691–701.
8. Fernández A, Sorokin A, Thompson PD. Corneal Arcus as Coronary Artery Disease Risk Factor. Atherosclerosis 2007;193:235–40.
9. Morelande MR, Iskander DR, Collins MJ, Franklin R. Automatic Estimation of the Corneal Limbus in Videokeratoscopy. IEEE Transactions on Biomedical Engineering 2002;49:1617–25.
10. Iskander DR. A Parametric Approach to Measuring Limbus Corneae from Digital Images. IEEE Trans Biomed Eng 2006;53:1134–40.
11. Consejo A, Iskander DR. Corneo-Scleral Limbus Demarcation from 3D Height Data. Contact Lens and Anterior Eye 2016;39:450–7.
12. Park CY, Lee JK, Zhang C, Chuck RS. New Details of the Human Corneal Limbus Revealed With Second Harmonic Generation Imaging. Invest Ophthalmol Vis Sci 2015;56:6058–66.
13. Le Q, Cordova D, Xu J, Deng SX. In Vivo Evaluation of the Limbus Using Anterior Segment Optical Coherence Tomography. Transl Vis Sci Technol 2018;7:12.
14. Tan B, Graham AD, Tsechpenakis G, Lin MC. A Novel Analytical Method Using OCT to Describe the Corneoscleral Junction. Optom Vis Sci 2014;91:650–7.
15. Gemoules G. A Novel Method of Fitting Scleral Lenses Using High Resolution Optical Coherence Tomography. Eye Contact Lens 2008;34:80–3.
16. Vincent SJ, Alonso-Caneiro D, Collins MJ. Optical Coherence Tomography and Scleral Contact Lenses: Clinical and Research Applications. Clin Exp Optom 2019;102:224–41.
17. Radhakrishnan S, Rollins AM, Roth JE, et al. Real-Time Optical Coherence Tomography of the Anterior Segment at 1310 nm. Arch Ophthalmol 2001;119:1179–85.
18. Mäurer S, Asi F, Rawer A, et al. Konzept zur 3-D-Vermessung von Hornhautspendergewebe Mithilfe eines Klinischen OCT. Der Ophthalmologe October 2018.

19. Konstantopoulos A, Hossain P, Anderson DF. Recent Advances in Ophthalmic Anterior Segment Imaging: a New Era for Ophthalmic Diagnosis? Br J Ophthalmol 2007;91:551–7.
20. Hoare CAR. An Axiomatic Basis for Computer Programming. Commun ACM 1969;12:576–580.
21. Skrok M, Alonso-Caneiro D, Siedlecki D. Automatic Determination of Anterior and Posterior Corneal Limbi from OCT Images Based on Corneal Shape Analysis. In: Optical Coherence Imaging Techniques and Imaging in Scattering Media III. Vol 11078. International Society for Optics and Photonics; 2019:110781X.
22. Bergmanson JPG, Martinez JG. Size Does Matter: What Is the Corneo-Limbal Diameter? Clin Exp Optom 2017;100: 522-8.
23. LaRocca F, Chiu SJ, McNabb RP, et al. Robust Automatic Segmentation Of Corneal Layer Boundaries in SDOCT Images Using Graph Theory and Dynamic Programming. Biomed Opt Express 2011;2:1524–38.
24. Skrok MK, Siedlecki D, Alonso-Caneiro D. Precise Geometry of the Anterior Chamber of the Eye by Means of OCT Imaging. Photonics Letters of Poland 2018;10:67–9.
25. Ortiz S, Siedlecki D, Grulkowski I, et al. Optical Distortion Correction in Optical Coherence Tomography for Quantitative Ocular Anterior Segment by Three-Dimensional Imaging. Opt Express 2010;18:2782–96.
26. Consejo A, Iskander DR. Determining the Position of Limbus Corneae from Anterior Eye Surface Topography. Invest Ophthalmol Vis Sci 2015;56:1965–1965.
27. Sakata LM, Lavanya R, Friedman DS, et al. Assessment of the Scleral Spur in Anterior Segment Optical Coherence Tomography Images. Arch Ophthalmol 2008;126:181–5.
28. Passing H, Bablok W. A New Biometrical Procedure for Testing the Equality of Measurements from Two Different Analytical Methods. Application of Linear Regression Procedures for Method Comparison Studies in Clinical Chemistry, Part I. J Clin Chem Clin Biochem 1983;21: 709–20.

29. Kohnen T, Thomala MC, Cichocki M, Strenger A. Internal Anterior Chamber Diameter Using Optical Coherence Tomography Compared with White-to-White Distances Using Automated Measurements. J Cataract Refract Surg. 2006;32:1809-13.
30. Baumeister M, Terzi E, Ekici Y, Kohnen T. Comparison of Manual and Automated Methods to Determine Horizontal Corneal Diameter. J Cataract Refract Surg. 2004;30:374-80.
31. Prospero Ponce CM, Rocha KM, et al. Central and Peripheral Corneal Thickness Measured with Optical Coherence Tomography, Scheimpflug Imaging, and Ultrasound Pachymetry in Normal, Keratoconus-Suspect, and Post-Laser in Situ Keratomileusis Eyes. J Cataract Refract Surg 2009;35:1055–62.
32. Grewal DS, Brar GS, Grewal SPS. Assessment of Central Corneal Thickness in Normal, Keratoconus, and Post-Laser in Situ Keratomileusis Eyes Using Scheimpflug Imaging, Spectral Domain Optical Coherence Tomography, and Ultrasound Pachymetry. J Cataract Refract Surg 2010;36:954–64.
33. Savini G, Carbonelli M, Barboni P, Hoffer KJ. Repeatability of Automatic Measurements Performed by a Dual Scheimpflug Analyzer in Unoperated and Post-Refractive Surgery Eyes. J Cataract Refract Surg 2011;37:302–9.
34. Fan Gaskin JC, Patel DV, McGhee CNJ. Acute Corneal Hydrops in Keratoconus - New Perspectives. Am J Ophthalmol 2014;157:921–8.
35. Ang M, Baskaran M, Werkmeister RM, et al. Anterior Segment Optical Coherence Tomography. Prog Retin Eye Res 2018;66:132–56.
36. Werner L, Lovisolo C, Chew J, et al. Meridional Differences in Internal Dimensions of the Anterior Segment in Human Eyes Evaluated with 2 Imaging Systems. J Cataract Refract Surg 2008;34:1125–32.

37. Rubin A. Short-Term Variation in Ocular Anterior Chamber Angle Using Scheimpflug Photography. S Afr Optom 2010;69:35–48.

Figures

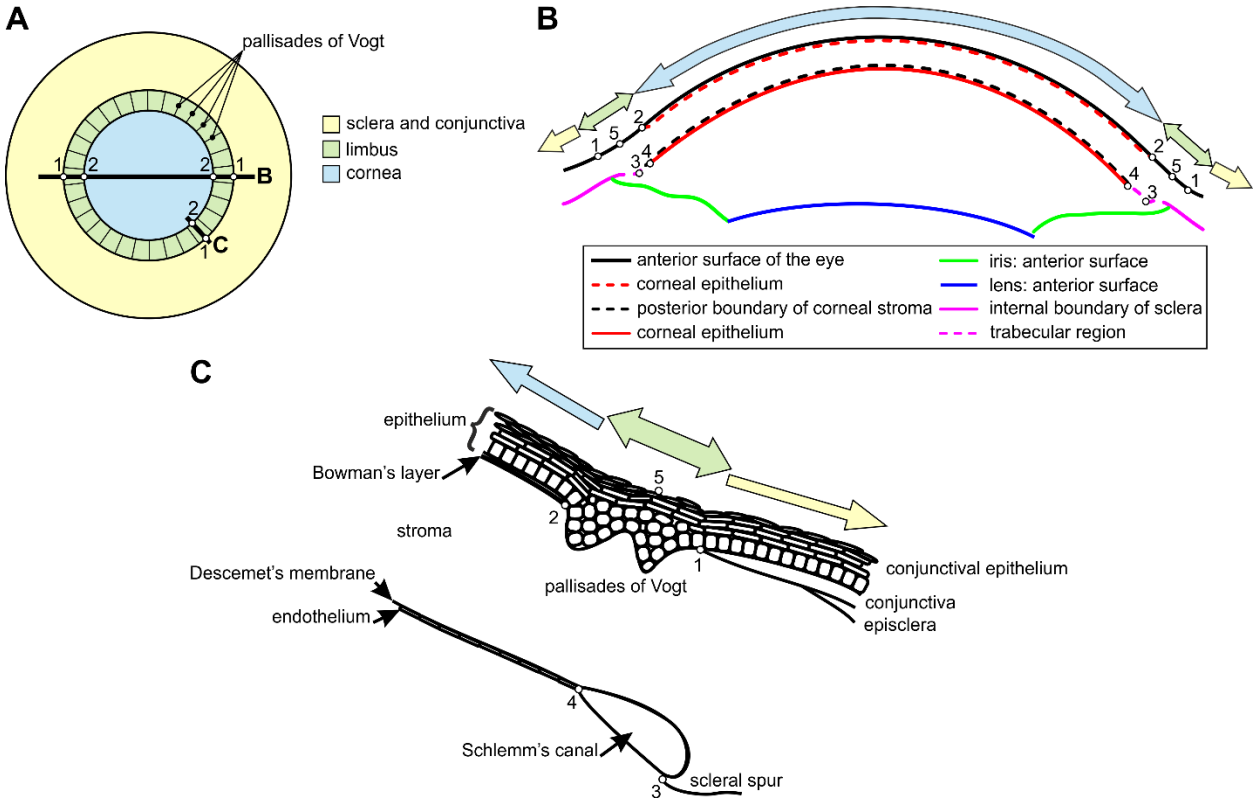

Figure 1. (A) Diagram of the corneal, limbal and scleral areas that can be viewed from the front of the eye. Black lines note the sections B and C explained in the corresponding diagrams. **(B)** Cross-sectional view of the anterior segment with its structures listed in the frame. **(C)** Schematic presentation of details of the limbus area. The limbal area is anatomically confined by the following points: peripheral boundary point of Vogt's palisades (marked with 1), the most peripheral point of Bowman's layer (2), the peripheral point of the corneal endothelium (3) and the scleral spur (4). Point of the most extreme change in the local curvature (marked with 5) is located between points (1) and (2). This point can be identified as the corneoscleral sulcus.

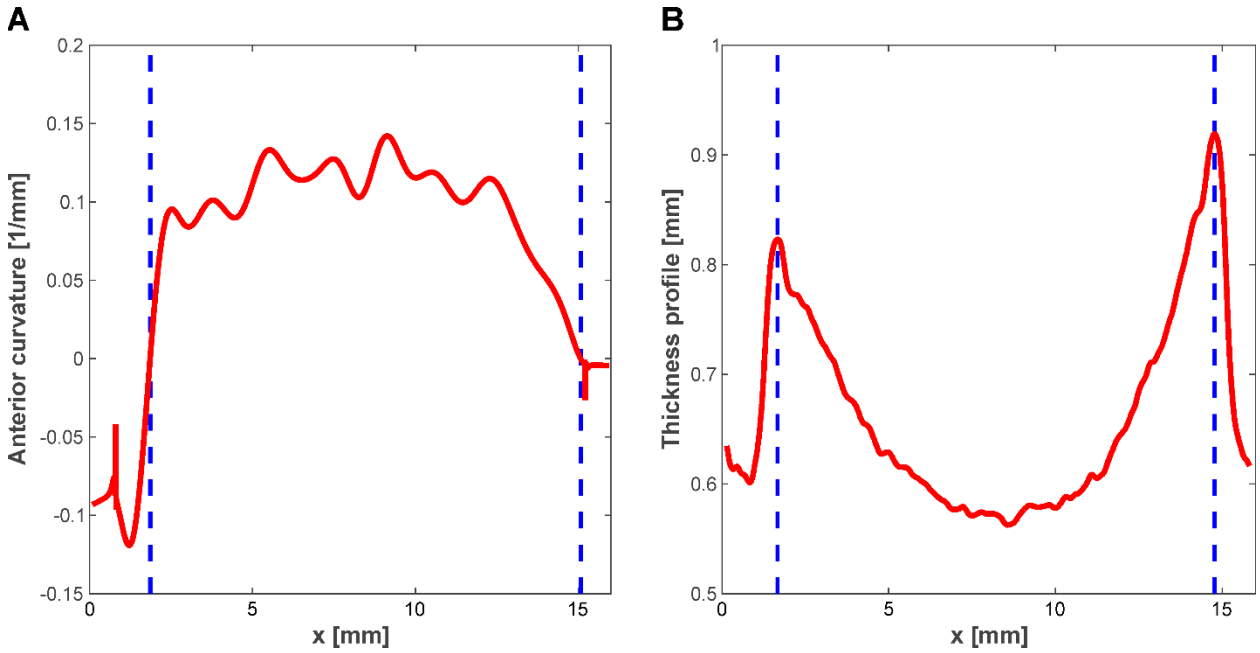

Figure 2. (A) An exemplary OCT image of the whole anterior segment captured by means of the Casia 2 OCT. Bars shown in the bottom left corner represent 1mm. (B) Presentation of the surfaces segmented from the raw OCT data (solid lines) and corrected from optical distortion (dashed lines). Iris and lens boundary data is shown for illustration purpose but not required for the limbus estimation.

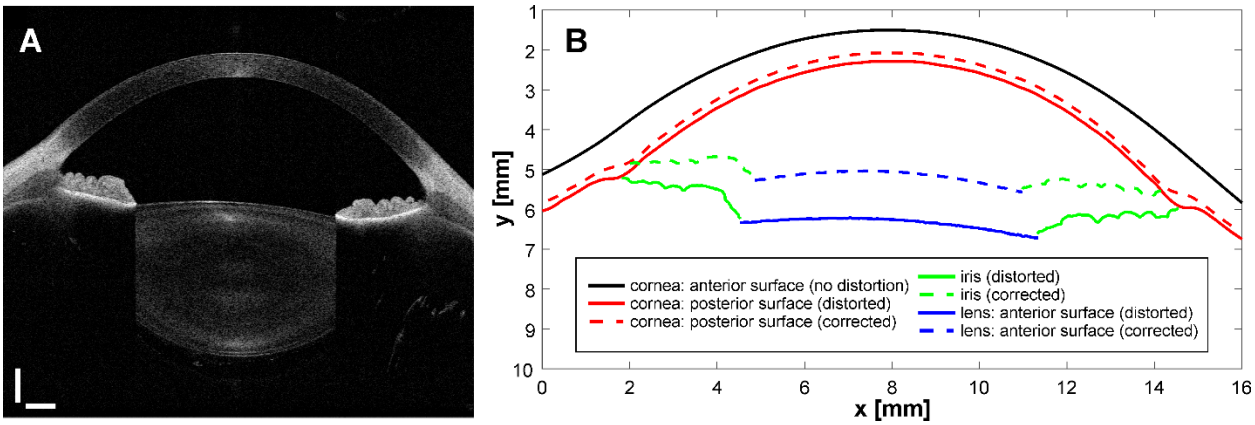

Figure 3. (A) Curvature profile of the anterior ocular surface obtained from the real OCT data. Red dashed lines indicate the local curvature equal to zero. (B) Thickness profile of the cornea. Red dashed lines indicate the local maxima of the thickness profile.

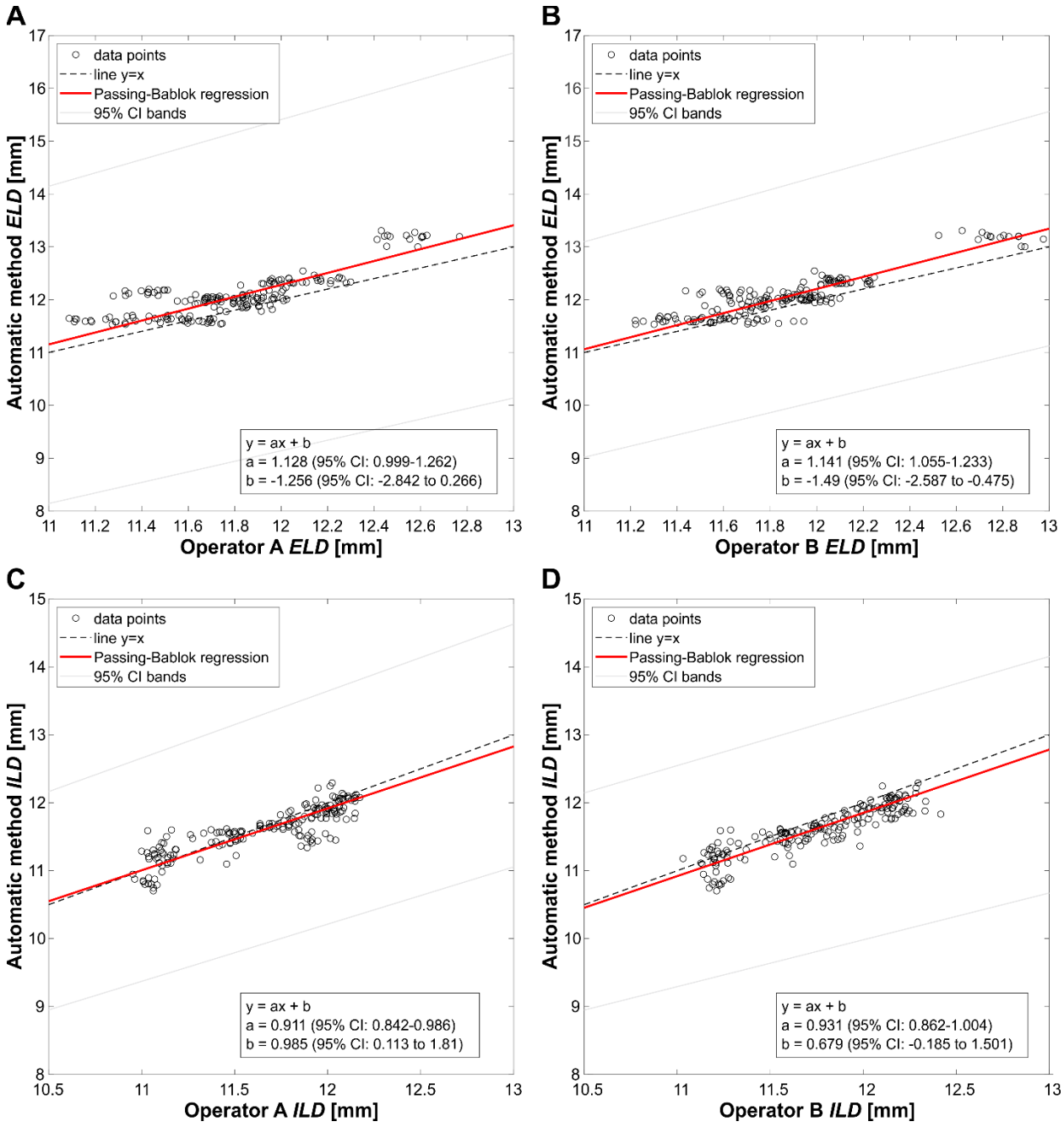

Figure 4. Passing-Bablok regression graphs for *ELD* (top row) and *ILD* (bottom row) calculated for the proposed automatic method and the manual identification of the limbal points by observer A (A,C) and by observer B (B,D).

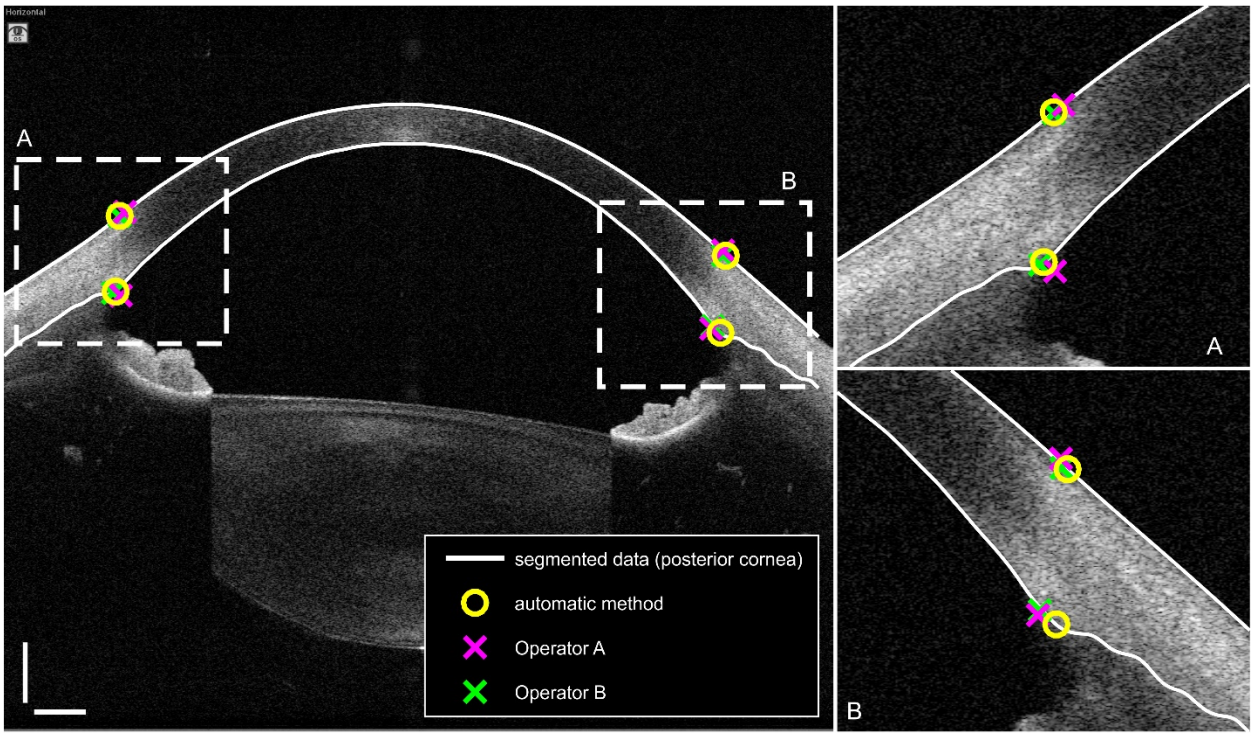

Figure 5. Comparison of results of subjective and automatic limbal points estimation on the example of the OCT data captured for Subject 6. The whole tomogram (raw data, uncorrected from optical distortion) with marked points obtained by manual identification (x) and automatic method (o). Bars shown in the bottom left corner represent 1 mm. The areas in the rectangles are magnified in the insets (A) and (B).